Combustion and Flame 159 (2012) 1832–1839

Contents lists available at SciVerse ScienceDirect

Combustion and Flame

journal homepage: www.elsevier.com/locate/combustflame

MILD combustion in diffusion-controlled regimes of Hot Diluted Fuel

M. de Joannon [a,*], G. Sorrentino [b], A. Cavaliere [b]

[a] Istituto di Ricerche Sulla Combustione, C.N.R., Piazzale Tecchio, No. 80, 80125 Naples, Italy
[b] Dipartimento di Ingegneria Chimica, Università Federico II, Piazzale Tecchio, No. 80, 80125 Naples, Italy

ARTICLE INFO

Article history:
Received 26 July 2011
Received in revised form 9 January 2012
Accepted 20 January 2012
Available online 9 February 2012

Keywords:
MILD combustion
Reactive structure
Diffusive layer
Combustion regimes

ABSTRACT

Reactive structures have been characterized in a steady laminar, unidimensional mixing layer on a dense grid of parameters in moderate or intense low-oxygen dilution (MILD) combustion conditions with hot and diluted fuel. The structures have been studied in terms of temperature and heat release profiles in a mixture fraction space for various ranges of stretch rates and for two reference pressures (1 and 10 bar) using a standard code and standard kinetic scheme.

In the analysis of reactive structure three synthetic characteristics have been pointed out in previous works as discriminative for the occurrence of different combustion regimes. Such characteristics are the thickness of the oxidation structures, the presence/absence of a pyrolysis region and the correlation/no correlation of the regions of maximum heat release with those at which the mixture is stoichiometric. Following the same criteria, maps of regimes have been built up on a inlet fuel temperature – temperature increase plane for fixed stretch rates and different pressures.

It has been pointed out that in diffusion controlled regimes of Hot Diluted Fuel, analysed in this paper, MILD combustion conditions are characterized by flame thickening and pyrolysis depression, which are also typical of flameless combustion. In addition, the region of maximum heat release has a generally high level of correlation with the stoichiometric regions. Thus, MILD combustion regime differs from MILD combustion regime found in other diffusion controlled regimes where the region of maximum heat release is generally not correlated with the stoichiometric regions. In the case presented in this paper, only a second solution, corresponding to a very low conversion occurring in a very wide stretch-rate range, shows no correlation between heat release and stoichiometric mixture fraction. This behavior has been attributed to the oxidative pyrolysis of methane.

At atmospheric pressure, the flameless characteristics extend to a low level of preheating, provided that the fuel is diluted, with a consequently low level of temperature increase, thus confirming that MILD and flameless regimes are not coincident in all possible feeding conditions.

In general, the results obtained in these Hot-Fuel-Diluted-Fuel conditions are consistent with and extend those reported in the literature for Hot-Oxidant-Diluted-Fuel, Hot-Oxidant and Diluted-Fuel conditions, supporting the assertion that these inlet parameters are a suitable choice for the definition of MILD combustion.

1. Introduction

In a survey of potential solutions for the mitigation of environmental problems, moderate or intense low-oxygen dilution (MILD) combustion represents a flexible and clean process that offers a trade-off between the optimization of fuel conversion and efficiency while avoiding drastic changes in the configuration of traditional plants [1].

MILD combustion has been rigorously defined as a process for which "the inlet temperature of the reactant mixture is higher than mixture self ignition temperature whereas the maximum allowable temperature increase with respect to inlet temperature during combustion is lower than mixture self ignition temperature" [2]. In other words, MILD combustion occurs when highly pre-heated and very diluted reactants are combined; thus, it refers to well-identified range of inlet parameters. From a practical point of view, such conditions can be obtained in several ways according to the typologies of the processes and systems involved. For example, premixed fuel/air mixtures can be ignited by hot products via internal or external gas recirculation in a combustion chamber. In this case, experimental [3] and numerical [4] tests that were carried out on a steady unidimensional diffusive layer demonstrated an extension of the reactive regions by increasing the temperature and dilution up to the point where the reaction zone overcomes the stagnation point. This characteristic justifies the classification of the relative reactive structure as Homogeneous Charge Diffusion Ignition (HCDI) [4].

* Corresponding author. Fax: +39 081 2391709.
E-mail address: dejoannon@irc.cnr.it (M. de Joannon).

0010-2180/$ - see front matter © 2012 The Combustion Institute. Published by Elsevier Inc. All rights reserved.
doi:10.1016/j.combustflame.2012.01.013

The analysis of the steady diffusion layer obtained from a fuel flow impinging on an oxidant jet requires a higher level of accuracy with respect to the premixed case because various types of conditions must be considered to fit the MILD combustion feed parameters. Furthermore, in such configurations, the fuel and/or the oxidant can be diluted and pre-heated, resulting in four combinations that yield different reactive structures. Experiments carried out under specific conditions [3,5–7] demonstrated unusual behavior. For example, ignition kernels were observed in conjunction with mixture fraction regions where they were not expected to be. In this framework, a systematic analysis of the classification of the phenomenology occurring in the different configurations was examined. Hot-Oxidant-Diluted-Fuel fed conditions, typical of applications where low calorific value fuels are used, were previously analyzed for both low and high molecular weight paraffins [8,9] as well as hydrogen [12,13] and their mixture with hydrogen [10,11]. It was noted that, in MILD combustion regimes, the reactive structure does not exhibit the characteristics of a standard diffusion flame. It widens significantly, whereas the typical pyrolytic region disappears. Simultaneously and remarkably, the position of the oxidative structure in mixture fraction space is not correlated to the location of the stoichiometric mixture fraction. It shifts toward the hot side, in the region of the lean mixture fractions, whereas the stoichiometric mixture fraction moves in the direction of the diluted reactants. This structure supports the occurrence of the Hot-Diluted-Diffusion-Ignition process. Results obtained for the Hot-Oxidant-Diluted-Oxidant configuration confirm the extension of the mixture fraction region that is covered by the reaction and the disappearance of the pyrolysis region. However, both the reactive region and the stoichiometric mixture fraction shift toward the hot and diluted reactant, which is the oxidant jet in this case. Therefore, no correlation between the maximum reaction activity and the stoichiometric mixture fraction occurs only in the very diluted case [9].

The present work aims to conclude the categorization and characterization of the reactive structures in the diffusive configuration, dealing with a fed condition corresponding to the Hot-Fuel-Diluted-Fuel counter flowing jets. Any other combination of the dilution and heating of not premixed reactants can be traced back to one of the cases analyzed in the past [8,9] or in this paper.

Processes controlled by Hot-Fuel-Diluted-Fuel oxidation can occur locally in several practical systems. Examples include aspects of coal combustion and low heating value fuel oxidation. In the first example, gasified diluted products can be oxidized by the fresh air. In the second example, the oxidation occurs in the downstream region of the system, where reformed low calorific value fuel is produced by thermo-chemical processes from raw materials. The indirect combustion fuel is injected into the internal recirculation zone (i.e., the flue gas region where oxygen is completely absent) and prepares the fuel mixture for the following oxidation in Hot-Fuel-Diluted-Fuel conditions.

The analysis has been carried out following the same approach as the two previous companion papers on Hot-Oxidant-Diluted-Fuel [8] and Hot-Oxidant-Diluted-Oxidant [9,10] conditions. This approach consists of detailed simulations of the thermochemical patterns in a dense grid of input parameters synthetized in regimes diagrams, and it differs from the other approaches only in the inlet conditions. Therefore, the results are tightly comparable with one another and the discussion of their implications extends the conceptual framework that was previously outlined.

2. Formulation of the problem and the numerical method

The structure of the reaction zones developing in a steady unidimensional diffusive layer was analyzed by considering the opposed jets configuration. The system is schematized in Fig. 1. The Hot-Fuel-Diluted-Fuel [9] conditions refer to a pre-heated and diluted methane–nitrogen flow, characterized by an inlet temperature (T_0), velocity (v_0) and a fuel molar fraction (X_f) that is fed toward an opposed flow of air at ambient temperature (T_{in}). The flow rates of the opposed jets were set in such a way that their kinetic energies are equal, meaning that the stagnation point in frozen conditions always occurs in the middle of the two inlet sections in each condition considered. Numerical analysis was carried out using the Oppdif module of the ChemKin [15] package. A mixture-averaged formula has been used for diffusion velocities by including also the thermal diffusion. An evaluation of the various reaction mechanisms present in literature [16–19] indicated that they have equivalent predictive capability on the reactive structure in the condition considered. This question was discussed in the previous work [8]. To ensure correspondence with the previous papers [4,8,9], GRI 3.0 was chosen in the numerical analysis described below.The structure of the reactive zone was analyzed by following the temperature (T) and heat release rate ($\dot{h}$) profiles as a function of the mixture fraction (Z). The mixture fraction only depends on the inlet conditions of both flows and allows for following the reactive structure in dependence of the local composition [20]. The advantage of describing the behavior of reactive structure in the mixture fraction space with respect to other parameters such as local equivalence ratio, has to be ascribed to the independence of Z on the fuel stoichiometry. Such an independency enables a deeper analysis of the reactive structures and an easier evaluation of their variation with respect to fed composition, as already shown in previous works. However, it is simple to obtain the trend as function of local equivalence ratio due to its simple relation with mixture fraction [21]. For the standard inlet conditions (corresponding to undiluted jets and $T_{in} = T_0 = 300$ K), T and $\dot{h}$ profiles were reported in Fig. 1 with solid and dashed lines, respectively.From $Z = 0$ and $T_{in} = 300$ K, the temperature rapidly increases up to a maximum of approximately 2220 K at a stoichiometric value of $Z = Z_{st} = 0.055$. Hereafter, T smoothly decreases as Z increases, reaching T_0 at $Z = 1$. From $Z = 0$, the related $\dot{h}$ sharply increases up to a maximum that occurs at the location of the maximum temperature at $Z_{st} = 0.055$. This trend supports the prevalence of exothermic reactions that mainly lead to the formation of intermediate or to products of oxidation. The $\dot{h}$ value then drops toward a negative minimum, which occurs at approximately $Z = 0.08$. It becomes zero for $Z = 0.17$ and remains at this value until $Z = 1$. The range of Z corresponding to the negative values of $\dot{h}$ identifies the region where endothermic reactions dominate. It is worth noting for the following analysis that the stoichiometric mixture fraction, equal to 0.055 in the undiluted case, shifts toward higher Z values as the dilution increases. This phenomenon is clearly seen in Fig. 2, where Z_{st} has been reported as function of the fuel molar fraction in the combustible jet.Detailed simulations were performed over wide range of both T_{in} and dilution of the fuel jet

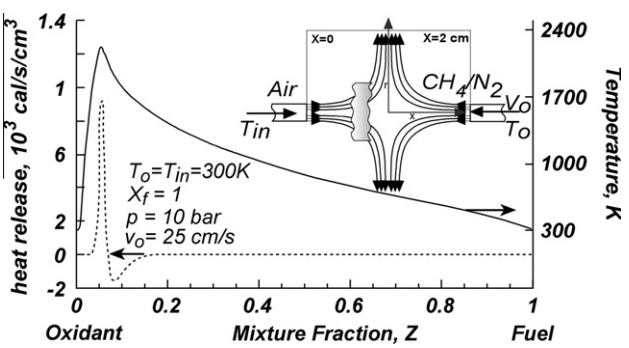

Fig. 1. Schematization of steady unidimensional diffusive layer configuration.

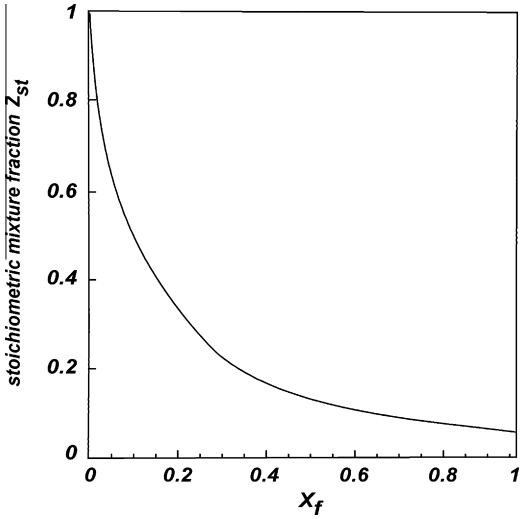

Fig. 2. Dependence of Z_{st} on fuel molar fraction in a combustible jet.

and strain rate $K_0 = \frac{v_0}{D}$ in adiabatic conditions, corresponding to 1 bar and 10 bar.

It has to be highlighted that the chosen configuration also aims to reproduce the reactive structures both on macro scale and on local scale. In the latter case it represents what occurs in a reactive structure locally present in a real system of combustion.

3. Results

The effects of dilution and pre-heating of the fuel flow can be seen at a glance by analyzing the synopsis of the temperature and heat release profiles reported in Figs. 3 and 4. In Fig. 3, the T (upper part) and $\dot{h}$ (lower part) profiles, computed for a pre-heating temperature of 1400 K, $v_0 = 100$ cm/s and $p = 10$ bar, are reported as a function of Z on curves parametric in X_f, over a range from 1 to 0.02. Both T and $\dot{h}$ are represented by solid lines that increase their thickness with X_f. The dots reported on the heat release curves indicate the value of $\dot{h}$ at Z_{st} for each X_f considered. On the same figure, the frozen temperature is also reported with a dashed line. The temperature profile obtained for $X_f = 1$, i.e., when no dilution is considered, is very similar in shape to the one reported for standard conditions in Fig. 1, although in this case, T reaches a higher maximum value of 2340 K for $Z = 0.053$, due to fuel pre-heating. The temperature then decreases down to $T_0 = 1400$ K for $Z = 1$. It is interesting to highlight that the frozen temperature shows an opposite trend with respect to T because it increases with Z. The $\dot{h}$ profile at $X_f = 1$ sharply increases up to an absolute maximum at $Z = 0.053$. It then decreases and exhibits a small shoulder at $Z = 0.062$, which is slightly higher than the $Z_{st} = 0.055$ that makes the oxidative region slightly larger toward a higher Z. This difference also results in a shift of the pyrolytic region. In fact, the minimum of $\dot{h}$ occurs at $Z = 0.1$, then it comes back to zero at $Z = 0.45$. Increasing fuel dilution enhances the differences with respect to the standard conditions. For $X_f = 0.7$, the maximum of T shifts toward a higher Z ($Z = 0.089$), very close to $Z_{st}^{X_f=0.7} = 0.0925$. The subsequent temperature decrease is slightly smoother than that observed in the absence of dilution. Consequently, the oxidative region in the related $\dot{h}$ profile shifts and widens. Again, it is characterized by the presence of a positive maximum at $Z = 0.089$ (which is slightly lower than $Z_{st}^{X_f=0.7}$) and by a more pronounced shoulder at $Z = 0.105$. The pyrolytic region enlarges slightly as Z increases, although the main effect of dilution is a decrease of the absolute value of the minimum $\dot{h}$. This behavior is even more

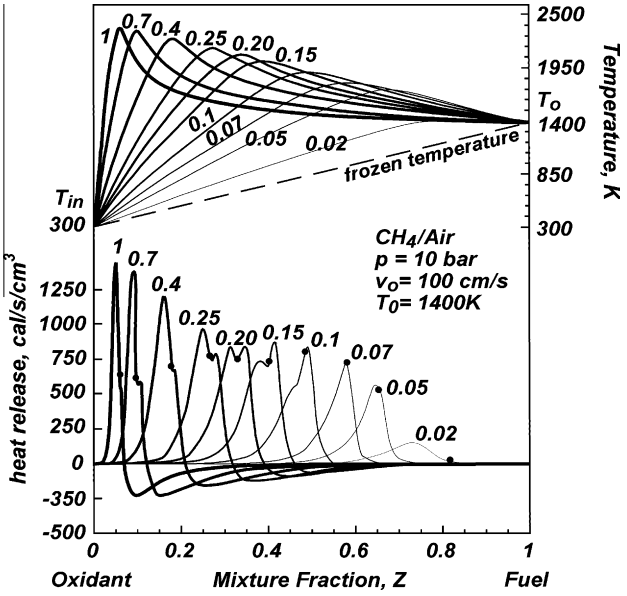

Fig. 3. T and $\dot{h}$ vs. Z, parametric on X_f at $p = 10$ bar.

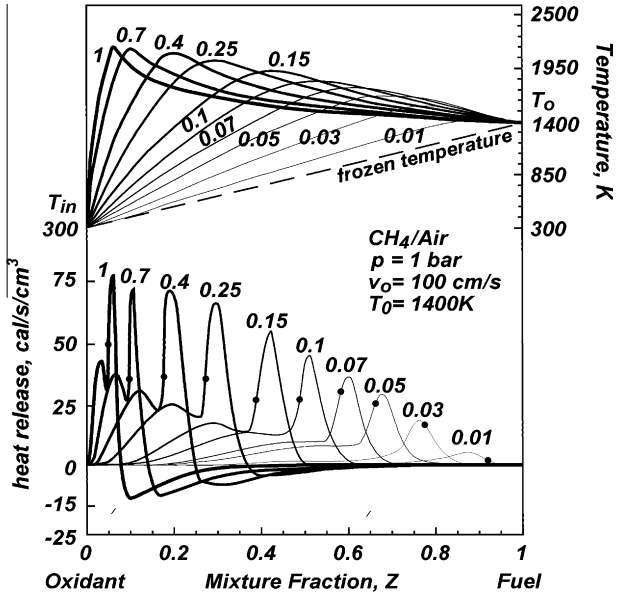

Fig. 4. T and $\dot{h}$ vs. Z, parametric on X_f at $p = 1$ bar.

pronounced when decreasing X_f, which makes the pyrolytic region vanish for X_f values lower than 0.1.

The evolution of the oxidative structure becomes more complex when varying the fuel dilution.The reactive structure continues to shift toward a higher Z following the shift of Z_{st} by decreasing X_f.The most relevant effect of the dilution increase is the evolution of the shoulder at the right side of the maximum of $\dot{h}$. For $X_f = 0.25$, this shoulder gains in magnitude and becomes a relative maximum that reaches the same value of the first maximum for $X_f = 0.2$. A further decrease of X_f makes the second peak the largest. The first peak, in turn, slowly reduces to be embedded in the remaining structure for $X_f = 0.07$. Simultaneously, a significant flame thickening occurs while the pyrolytic region disappears. The increase of dilution level makes the part of the mixing layer where the composition allows for ignition, shift towards a region characterized by a higher frozen temperature.For still higher dilution levels, $\dot{h}$ profiles exhibit only a single maximum that decreases in intensity with X_f.

However, the oxidative region moves toward a higher Z, and this shift occurs in the same direction with respect to Z_{st}. For example, the maximum $\dot{h}$ computed for $X_f = 0.05$ occurs at $Z = 0.65$, whereas $Z_{st}^{X_f=0.05} = 0.66$.At 1 bar, the T and $\dot{h}$ profiles retain their main characteristics, although minor differences can be found (Fig. 4). Also, in this case, $\dot{h}$ profiles show two maxima from $X_f = 1$ to 0.15. From $X_f = 0.10$, the first maximum turns into a shoulder on the left side of the curve that persists up to $X_f = 0.05$. The oxidative region shifts toward a higher Z. No substantial differences can be identified in the evolution of the pyrolytic region. It is present at $X_f = 1$ and then it decreases up to disappear at $X_f = 0.15$. T and $\dot{h}$, as reported so far, refer to a steady state solution with a significant fuel conversion. However, for most of the fuel temperature range explored, the system has two different steady states, having strongly different oxidative structures. In Fig. 5, the $\dot{h}$ profiles obtained for the two steady states at $T_0 = 1200$ K, $X_f = 0.5$ and $p = 10$ bar are shown. The solid line represents the solution corresponding to a high fuel conversion that is very similar to the ones analyzed above.The profile related to the very low fuel conversion, reported in Fig. 5 with a dashed line, is very different. Low fuel conversion solution is a stable solution that is obtainable in properly inlet conditions. In fact, while in the standard case, the methane results totally converted in the oxidation region, in the low conversion solution, the methane conversion decrease monotonically by increasing mixture fraction. In this case, the heat is released at very high Z values. The heat release rate peaks at $Z = 0.88$. Moreover, the characteristic values reached by heat release rate in this case are an order of magnitude lower than in the case of the high fuel conversion. In contrast with the high fuel conversion profile, the dashed line shows a reactive structure covering a wide range of Z and is totally uncorrelated with the stoichiometric mixture fraction. In fact, it occurs at the fuel side of the stagnation point.The double stable solutions are present over a wide range of T_0 and dilution, and this characteristic is also maintained at different values of K_0, as indicated by the analysis of Fig. 6.This figure reproduces the peak values of $\dot{h}$ as a function of K_0 up to 300 s^{-1}. These values were computed at $X_f = 0.7$, $p = 1$ bar for three different T_0. In each plot, the higher branch indicates $\dot{h}$ related to the high conversion solution, whereas the lower branch indicates $\dot{h}$ corresponding to the low fuel conversion. Both the low and high conversion steady states are obtained for each value of K_0, up to approximately 250 s^{-1}. For higher values of K_0, only the low conversion solution was found. Moreover, the low conversion solution has heat release increasing by increasing T_0, from $T_0 = 1200$ K to $T_0 = 1600$ K.Based on the typology of the heat release profiles reported in Figs. 3 and 4, an overall characterization of the combustion regimes occurring under the different feed conditions was carried out. This analysis follows the same approach that was applied in the previous papers, related to Hot-Oxidant-Diluted-Fuel and Hot-Oxidant-Diluted-Oxidant inlet conditions. Thus, it produces a map of behavior as a function of the inlet parameters, i.e., T_0 and the dilution level. The latter factor is taken into account by considering the maximum allowable temperature increment ΔT for the corresponding feed conditions. The T_0–ΔT plane obtained for $T_{in} = 300$ K, $K_0 = 50$ s^{-1} and $p = 10$ bar is reported in Fig. 7. In both cases, T_0 ranged from 600 K to 2400 K, whereas ΔT ranged from 600 K to 2000 K. At $p = 10$ bar (Fig. 7), the map is divided in four main regions that are analogous to the maps outlined for the Hot-Oxidant-Diluted-Fuel and Hot-Oxidant-Diluted-Oxidant cases. The thresholds between the combustion regions have been obtained by analyzing the shape or intensity of temperature and/or of heat release profiles. The region corresponding to the lowest T_0 and ΔT, in the lower-left part of the map, identifies the conditions at which "no combustion" takes place. In this case the temperature profile obtained coincides with frozen temperature and the heat release rate is zero in the whole range of mixture fraction. It extends up to $T_0 = T_{in}$, which is the ignition temperature of methane at $p = 10$ bar. In the same range of T_0, an increase of ΔT leads to the combustion regime sustained by the "feed-back" of chemical species and heat from the flame front, such as is observed in systems working in traditional conditions. In this case, a flame structure that is typical of diffusive flames stabilizes. The oxidative region, centered near Z_{st}, is then followed by a pyrolytic region. The feed-back combustion progressively approaches the high temperature combustion by increasing the pre-heating temperature of fuel. In this case, the structure of the flame enlarges over a wider range of Z while

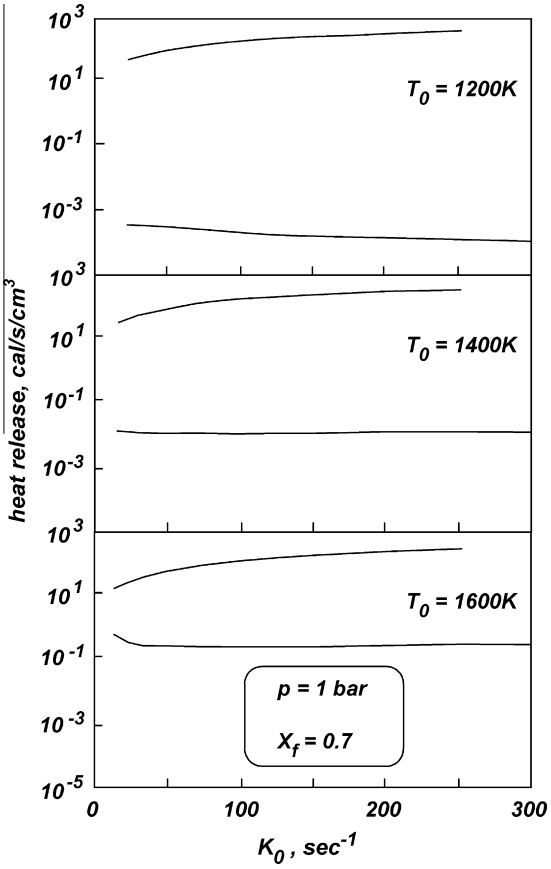

Fig. 6. $\dot{h}$ vs. K_0 for different inlet temperatures at $X_f = 0.7$.

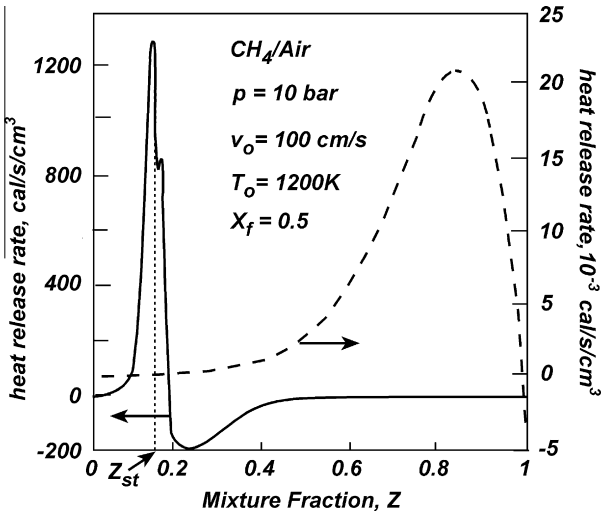

Fig. 5. $\dot{h}$ profiles for high and low conversion solution at $T_0 = 1200$ K and $X_f = 0.5$.

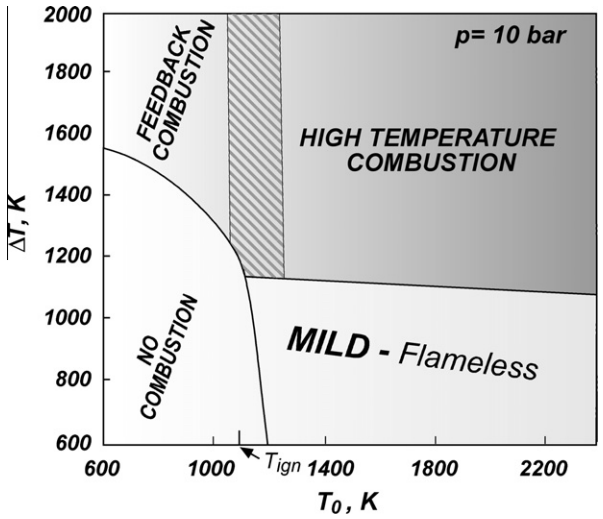

Fig. 7. Combustion regimes at $p = 10$ bar, $T_{in} = 300$ K and $K_0 = 50\ s^{-1}$.

keeping the main features of feed-back combustion structures. The presence of the dashed region express that there is a gradual shift between "feed-back" and high temperature regimes without a threshold effect. This phenomenon is different from the identification of the transitional region in the Hot-Oxidant-Diluted-Fuel case [8] where the transitional region was associated with the existence of multiple steady states.

From the high temperature combustion regime, a decrease of ΔT leads to a further widening of the reactive structure to reach the MILD combustion area, where the pyrolytic region is no longer noticeable in the reactive structure. These two characteristics are related to "flameless" combustion, as indicated by the map.

To better understand the change of reactive structure in the shift from high temperature combustion to MILD, analysis on the partial heat release rates related to single species has been carried out by considering the chemical species as markers of the different combustion phases. A preliminary analysis has suggested a number of the key species that most significantly contribute to the magnitude of the global heat release in the various steps of the process.In Figs. 8 and 9, heat release profiles related to the production of CO, CO_2, C_2H_2 and H_2O (computed at 1400 K, and 10 bar) have been reported for $X_f = 1$ and $X_f = 0.02$ (along with the overall $\dot{h}$).In particular, Fig. 8 indicates the heat release distribution in the Z coordinate for a system in which the fuel flow is not diluted and is pre-heated to 1400 K. The pressure is 10 bar and the strain rate is $50\ s^{-1}$. In the map of behavior, reported in Fig. 7, such conditions fall into the high temperature combustion region because no dilution and high inlet temperatures are considered. The global heat release, reported in black, extends into the Z range, from values near 0 to 0.2.The global $\dot{h}$ maximum value occurs in conjunction with Z, where H_2O, CO and CO_2 exhibit their maxima.For $Z > 0.054$, the heat release decreases, reaching a minimum negative value at $Z = 0.1$. Acetylene heat release mainly contributes to the negative region for the higher values of Z. In this region, the depletion of oxygen and the relatively high temperatures promote endothermic reactions, such as methane thermal decomposition or methyl radical recombination and dehydrogenation, which respectively lead to the formation of CH_3 and C_2H_2. The latter product strongly contributes to the negative value of $\dot{h}$, along with all the C_2 species that participate in the reaction channel that lead to the formation of C_2H_2.

Analysis of the partial heat release indicates that the structure of the oxidative region is complex, and several predominant phases that occur during the oxidation of CH_4 are recognizable in relation to the local composition of the mixture and temperature.

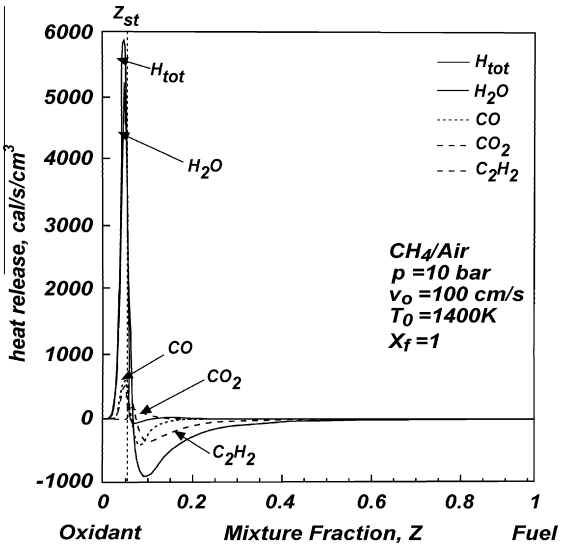

Fig. 8. Global heat release and heat release relative to selected species at $T_0 = 1400$ K and $X_f = 1$.

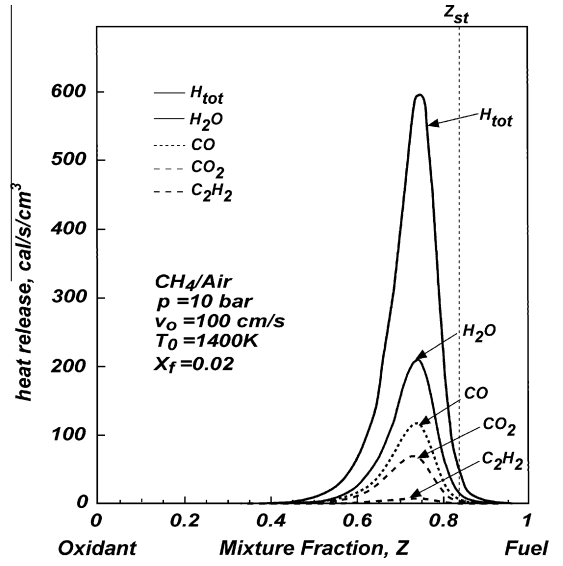

Fig. 9. Global heat release and heat release relative to selected species at $T_0 = 1400$ K and $X_f = 0.02$.

The heat release shown in Fig. 9 is indicative of the MILD combustion regime. The global heat release shows a single peak that occurs at a Z lower than the stoichiometric mixture fraction. Both the global $\dot{h}$ and the heat release relative to H_2O, CO, CO_2 and C_2H_2 show their maximum at $Z = 0.73$.

The low fuel content and the low heat release and temperature values do not favor the methyl radical recombination reaction to ethane, resulting in a depression in the formation of C_2 compounds. Furthermore, no predominant pyrolytic region is evident in the global heat release profile, and both the oxidation of methyl radicals to intermediate species and the full conversion of methane occurs almost in the same Z range. The heat release associated with these reactions compensates for and overcomes the heat detraction due to thermal decomposition and dehydrogenation reactions occurring in the same Z range.

The main result that can be inferred from the analysis of the heat release profiles reported in Figs. 8 and 9 is that the oxidative structure obtained in MILD combustion conditions has a uniform

structure that is different from the structure associated with high temperature combustion. This conclusion is in agreement with the nearly homogeneous temperature and concentration profiles that characterize MILD combustion [22].

A map of combustion regimes for $p = 1$ bar is shown in Fig. 10. It clearly indicates that the ranges of parameters corresponding to the different regimes change to some extent while keeping the characteristics of the four main regions. Compared to the case of $p = 10$ bar shown in Fig. 7, a new feature is the transitional zone that is present at this pressure between the feed-back combustion and the no-combustion region. The flame thickening and the absence of pyrolytic region justify the identification of such a transitional zone as "flameless" but the inlet temperatures that are lower that the ignition one, thus, not fitting the MILD combustion conditions by definition. The significance of this classification will be better clarified in the discussion.

4. Discussion

MILD combustion has been defined in the literature [1,2,22] on the basis of the feeding conditions. It is a combustion process in which the reactants are fed in such a way that the frozen temperature of the system is higher than the autoignition for part of the possible mixture fractions, and the dilution of the reactants mixture is high enough such that the maximum theoretical temperature increase is lower than the autoignition temperature increase with respect to room temperature.

The peculiar feeding conditions make it reasonable to expect that outstanding properties (e.g., flameless, noiseless, and pollutant free) should occur. Several attempts have been reported to show this assumption under all possible feeding configurations. Among these relevant for not premixed conditions are those that were obtained in counterflow conditions for different combinations of heating and dilution of the reactants [8,9].

It has been shown in previous papers that, when the two feeding conditions (dilution and pre-heating), are obtained separately for the two reactants, the local heat release spatial structure is quite different from the processes that are known as "diffusion flames". In fact, in contrast from diffusion flames, they are characterized by three outstanding characteristics:

– Pyrolysis depression.

– Flame thickening.

– No correlation of the stoichiometric and maximum heat release conditions.

All of these characteristics are signatures of a special situation that can occur in MILD combustion conditions. In particular, it is relevant that the control of the process relies on the heating of one reactant and not on the autocatalytic conditions generated by the heat released due to oxidation. This peculiarity has been emphasized by the use of a specific name when all of these characteristics occur: Hot-Diluted-Diffusion-Ignition (HDDI) [8].

In this context, it is straightforward to focus on the main result of this paper, which refers to the third and last kind of feeding of a counter-diffusion oxidation process in MILD conditions (Hot Fuel Diluted Fuel). This is a very peculiar process that is like the other ones reported in the previous papers but it does not coincide with a HDDI process in the whole range of occurrence.In fact, the pyrolysis depression and the flame thickening characteristics have been shown to occur in subregions in the regime diagrams reported in Figs. 7 and 10 approximately in the parameter range in which MILD combustion is defined. Instead, the third characteristic, i.e. the no correlation of the stoichiometric and maximum heat release conditions, is only occasionally present in a limited part of the domain. To clarify such a feature, the mixture fraction in Fig. 11 corresponding to the maximum heat release rate ($Z_{h\max}$) has been reported as a function of Z_{st} for Hot-Oxidant-Diluted-Fuel [8] and Hot-Fuel-Diluted-Fuel conditions. The no correlation of the stoichiometric and maximum heat release is clearly visible for the Hot-Oxidant-Diluted-Fuel conditions. As a matter of a fact, $Z_{h\max}$ is nearly coincident with Z_{st} up to a particular level of dilution. This relation ceases to hold true for higher Z_{st} because an increase of dilution (i.e. of Z_{st}) makes $Z_{h\max}$ decrease, meaning that Z_{st} and $Z_{h\max}$ move in opposite directions on the Z axis. The values of $Z_{h\max}$ for the configuration presented in this paper, Hot-Fuel-Diluted-Fuel, show a different behavior. This variable is nearly coincident with Z_{st} up to $Z_{st} = 0.66$ ($X_f = 0.05$). Only after this dilution level does $Z_{h\max}$ shift slightly with respect to Z_{st}. No correlation of the stoichiometric and maximum heat release conditions is not a novel characteristic in combustion processes because it has been identified in the ignition processes of turbulent non premixed flames [23].

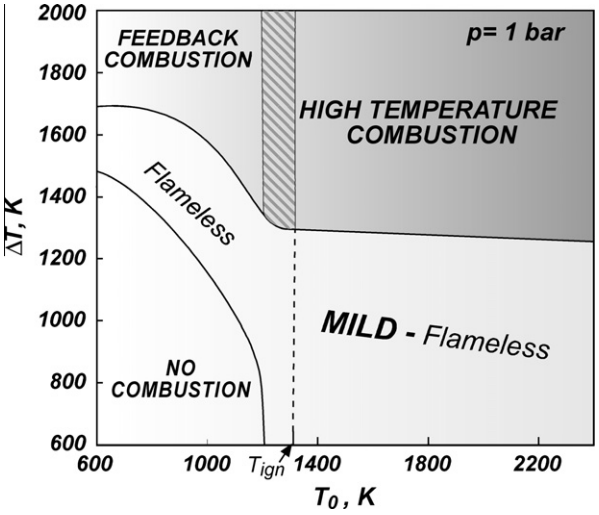

Fig. 10. Combustion regimes at $p = 1$ bar, $T_{in} = 300$ K and $K_0 = 50$ s^{-1}.

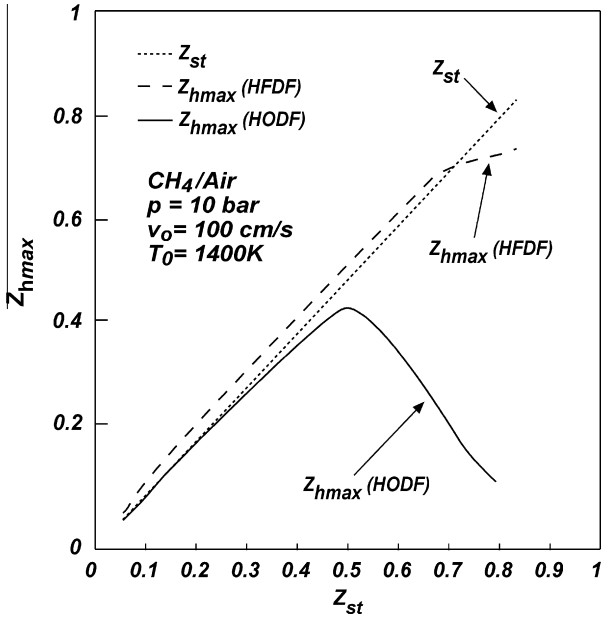

Fig. 11. Profiles of $Z_{h\max}$ as a function of Z_{st} for two different configurations at $p = 10$ bar, $T_{in} = 1400$ K and $K_0 = 50$ s^{-1}.

This study provides the first example of a non-perfect coincidence of MILD combustion conditions and Hot-Diluted-Diffusion-Ignition (HDDI) conditions. The data indicate that HDDI is a subregion of MILD combustion region. In fact, pyrolysis depression is a necessary condition to yield colorless products [24]. However, flame thickening is a necessary condition to support distributed flame processes. These two properties (colorless and distributed flame) have been frequently reported in relation to combustion regimes that are classified as flameless combustion [25]. In these regimes, both the typical "traditional" features of visible emissions and the "front-like" structure of oxidation disappear. Thus, these two properties (flame thickness and pyrolysis depression) are coincident with flameless properties; therefore, the domain over which they occur has been classified as flameless regimes.

Here it has been found the presence of the flame thickening/pyrolysis depression outside the MILD combustion region. In fact, for both pressure conditions, they also occur at inlet temperature lower than the autoignition one. This factor is clearly indicated in Fig. 10, where the "flameless" area extends in the narrow peninsula on the left side relative to the region where MILD combustion is defined. This feature is relevant to emphasize that the main effect of the dilution is to slow down the chemical kinetics of both pyrolysis and oxidation, as well as to lower the adiabatic flame temperature and the concentration of the reactants. To be more precisely, on one hand, the dilution effect slows all kinds of reactions (oxidation and pyrolysis), leading to flame thickening. On the other hand, the lowering of the concentration of the reactants exerts a more significant effect on the third order reaction, which controls CH_3 recombination, and on the post combustion reactions. CH_3 recombination is the main channel of C_2H_2 formation, in addition to other heavier compounds; therefore, its slower formation affects the entire downstream pyrolytic network. The post combustion zone, with radical recombination and CO oxidation, is also very sensitive to the partial pressure of the species, which is lowered significantly by dilution. Therefore, flame thickening can be explained by also taking this effect into account. In summary, flame thickening and pyrolysis depression are independent effects of dilution.This peninsula in the regime diagram is absent in the other counter-flow feeding condition that was analyzed in relation to the other MILD combustion conditions [8,9]. This difference is due to the effect of the dilution of the fuel on the stoichiometric value of the mixture fraction [22] in relation to the frozen temperature distribution. The higher the dilution, the higher the value of the stoichiometric mixture fraction, as indicated by Fig. 2. In this particular feeding condition, the shift of Z_{st} toward a higher Z value makes the Z_{st} correspond to an even higher value of the frozen temperature, as also indicated by Figs. 3 and 4. Thus, the lowering of the adiabatic flame temperature is partially compensated for by the increase of the frozen temperature. Conversely, for other diffusive controlled conditions analyzed elsewhere (Hot-Oxidant-Diluted-Fuel), the frozen temperature decreased toward higher mixture fraction values. Therefore, both the adiabatic temperature decrease and the frozen temperature lowering occur simultaneously so that the autocatalytic "classical" diffusion flame cannot occur, and eventually, only the autoigniting solution is possible. Thus, Hot-Oxidant-Diluted-Fuel refers to conditions that allow a significant reactant conversion toward oxidated products in autoigniting conditions. On the contrary, in the conditions discussed in this paper (Hot-Fuel-Diluted-Fuel), an autoignitive regime is present but only corresponds to a low level of conversion. This autoignitive regime has to be considered either the main or the secondary regime in terms of conversion in connection with the fluid-dynamic. Figure 6 indicates the autocatalytic regime disappears beyond a quenching threshold level whereas the autoignitive regime survives and eventually intensifies. A quenching threshold level exists for various feeding conditions and the shift from autocatalytic to autoignitive regime is affected by the stretch rate Even though the autoigniting solution is the only possible beyond the quenching stretch rate, it corresponds always to a fuel conversion relatively low. Fuel (hot and diluted) diffuses in a cold oxidant medium; therefore, it partially converts with the aid of oxygen that it meets in the diffusion. This conversion refers to a simple hydrogen extraction through H_2 and C_2H_6 formation (as demonstrated by species plots not reported here) enhanced by faintly exothermic reactions, similar to the one leading to the heat release curves in Figs. 3 and 4.

This type of process must mainly be considered an oxidative reforming process rather than a simple oxidation one. It is relevant in the preparation of the more effective oxidation process that takes place afterwards. In this respect, it is also important with regard to pollution because it depresses the pyrolytic recombination that can lead to the formation of heavier carbonaceous products. In contrast, pyrolytic recombination is relevant when fuel undergoes a high-temperature conversion in the absence of oxygen. This reaction only occurs at a much higher temperature relative to that at which low conversion activity occurs. As a matter of fact, pure pyrolytic reforming has been observed at temperature above 1900 K. This event has not been analyzed in detail here due to its irrelevance in the analysis of the MILD combustion process. This irrelevance is clear from the analysis of Fig. 9, where the heat release curve related to the recombination species C_2H_2 is negligible. In any case, it is clear that the two processes are not contiguous in the regime diagram and that they cannot be confused with one another.

5. Conclusions

The present paper concludes the overview on the basic possible steady reactive structures that can occur when fuel and oxidant flows variously diluted and pre-heated interact, showing the behavior of structures in the last fundamental case, identified as Hot-Fuel-Diluted-Fuel conditions.

In general, the results obtained in these Hot-Fuel-Diluted-Fuel conditions are consistent with and extend those reported in the literature for Hot-Oxidant-Diluted-Fuel [8], Hot-Oxidant and Diluted-Oxidant [9,14] conditions, supporting the assertion that these inlet parameters are a suitable choice for the definition of MILD combustion. Also in this case, maps of behavior have been built up on the basis of recognition of discriminative features that allow for identification of the different regime of combustion.It is worthwhile to note that the maps of behavior reported in the analysis of reactive structures are related to local conditions that occur in a MILD combustion chambers. As discussed, inlet temperature and maximum attainable temperature (i.e. the oxygen concentration at the inlet section) reported on the axes can be related to local or overall initial conditions according to either the system or the control volume considered. In the definition of MILD combustion such parameters have been properly chosen to univocally identify the initial conditions of reactants. Some authors prefer to consider the recirculation rate K_v [28,29] in place of inlet temperature to build up working map of operative burners, where K_v is defined as the ratio between the recirculated products and the sum of fresh air and fuel fed to the combustion system. Thus, K_v is a more restrictive parameter that does not allow for representation from basic point of view the effect related to dilution. On the other hand, having the proper indication the term K_v can be easily related to inlet temperature of the system. Indeed, initial temperature of mixed reactants is directly related to the recirculated flow.

An additional important consideration concerns the effectiveness of the kinetic mechanisms available in literature in the evaluation of fuel oxidation in diluted and pre-heated conditions. It has been verified across various conditions that kinetic mechanisms

are able to predict the general behavior of systems working in these conditions [8]. In this sense, they do not need further validation. The only consideration that has yet to be examined involves uncertainty in the position of the autoignition threshold. In this case, the kinetic mechanisms cannot be considered to be strictly equivalent [26]. Their tuning in the temperature range of MILD combustion has not been possible thus far because of a dearth of experimental results in these working conditions. Only recently have experimental results been obtained in a tubular flow reactor; these data confirm the need for revising the different ignition pathways with regards to their competition across various temperature ranges [27].

References

[1] M. de Joannon, P. Sabia, A. Cavaliere, MILD combustion, in: M. Lackner (Ed.), Handbook of Combustion, 2010, 237–256.
[2] A. Cavaliere, M. de Joannon, Prog. Energy Combust. Sci. 30 (4) (2004) 329–366.
[3] E. Mastorakos, A. Taylor, J. Whitelaw, Combust. Flame 102 (1–2) (1995) 101–114.
[4] M. de Joannon, A. Matarazzo, P. Sabia, P, A. Cavaliere, Proc. Combust. Inst. 31 (2) (2007) 3409–3416.
[5] C. Fotache, T.G. Kreutz, C.K. Law, Combust. Flame 108 (4) (1997) 442–470.
[6] Y. Liu, J. Most, P. Bauer, A. Claverie, Int. J. Min. Met. Mater. 16 (3) (2009) 278–284.
[7] K. Maruta, K. Abe, S. Hasegawa, S. Maruyama, J. Sato, Proc. Combust. Inst. 31 (1) (2007) 1223–1230.
[8] M. de Joannon, P. Sabia, G. Sorrentino, A. Cavaliere, Proc. Combust. Inst. 2 (2008) 3147–3154.
[9] M. de Joannon, P. Sabia, A. Cavaliere, HDDI MILD combustion, in: M. Lackner (Ed.), Alternative Ignition Systems, Process Eng Engineering GmbHWien, 2009, pp. 133–151.
[10] S. Chen, C. Zheng, Int. J. Hydrogen Energy 36 (2011) 15403–15413.
[11] A.F. Colorado, B.A. Herrera, A.A. Amell, Bioresour. Technol. 101 (2010) 2443–2449.
[12] S. Chen, H.F. Han, Z.H. Liu, J. Li, C.G. Zheng, Int. J. Hydrogen Energy 35 (2010) 4736–4746.
[13] S. Chen, J. Mi, H. Liu, C. Zheng, Int. J. Hydrogen Energy (2012), doi:10.1016/j.ijhydene.2011.12.039.
[14] M. de Joannon, G. Cozzolino, G. Sorrentino, P. Sabia, A. Cavaliere, Combust. Sci. Technol., in press, doi:10.1080/00102202.2012.664012.
[15] R. Kee, F.M. Rupley, J.A. Miller, M.E. Coltrin, J.F. Grcar, E. Meeks, H.K. Moffat, A.E. Lutz, G. Dixon-Lewis, M.D. Smooke Inc., San Diego, CA, 2000.
[16] J. Warnatz, U. Maas, R. Dibble, Combustion: Physical and Chemical Fundamentals, Modeling and Simulation, Experiments, Pollutant Formation, Springer Verlag, 2006. pp. 333–344.
[17] F. Williams. <http://web.eng.ucsd.edu/mae/groups/combustion/>.
[18] E. Ranzi, T. Faravelli, A. Frassoldati, A. Cuoci, CRECK Modeling. <http://creckmodeling.chem.polimi.it/kinetic.html>.
[19] G.P. Smith, D.M. Golden, M. Frencklach, N.W. Moriarty, M. Goldenberg, C.T. Bowman, R.K. Hanson, S. Song, W.C. Gardiner, V.V. Lissianski, Z. Qin. <http://www.me.berkeley.edu/gri_mech/>.
[20] A. Cavaliere, R. Ragucci, Prog. Energy Combust. Sci. 27 (5) (2001) 547–585.
[21] N. Peters, Proc. Combust. Inst. 21 (1988) 1231–1259.
[22] A. Cavaliere, M. de Joannon, R. Ragucci, in: D. Dunn-Rankine (Ed.), Lean Combustion: Technology and Control, Academic Press, San Diego, 2008, p. 55.
[23] E. Mastorakos, Prog. Energy Combust. Sci. 35 (1) (2009) 57–97.
[24] H. Tsuji, A. Gupta, M. Katsuki, High Temperature Air Combustion: From Energy Conservation to Pollution Reduction, CRC Press, Boca Raton, 2003. pp. 39–48.
[25] J. Wünning, J. Wünning, Prog. Energy Combust. Sci. 23 (1) (1997) 81–94.
[26] P. Sabia, M. de Joannon, A. Picarelli, A. Chinnici, R. Ragucci, Fuel 91 (1) (2012) 238–245.
[27] P. Sabia, M. de Joannon, R. Ragucci, A. Picarelli, A. Cavaliere, 10th International Conference on Combustion and Energy Utilization Programme, Mugla, Turkey, 2010.
[28] P. Li, J. Mi, Flow Turbul. Combust. 87 (2011) 617–638.
[29] M. Derudi, R. Rota, Proc. Combust. Inst. 33 (2011) 3325–3332.